DOI: 10.13009/EUCASS2023-059
Aerospace Europe Conference 2023 – 10TH EUCASS – 9TH CEAS

Design Study of a 30kN LOX/LCH4 Aerospike Rocket Engine for Lunar Lander Application

Ralf Stark[1⋆], *Sebastian Bartel*[2], *Florian Ditsche*[1] *and Thomas Esch*[2]

[1]*German Aerospace Center, Langer Grund, D-74239 Lampoldshausen, Germany*
[2]*FH Aachen - University of Applied Sciences, Bayernallee 11, D-52066 Aachen, Germany*
⋆Corresponding author

Abstract

Based on lunar lander concept EL3, various LOX/CH4 aerospike engines were studied. A distinction was made between single and cluster configurations as well as ideal and non-ideal contour concepts. It could be shown that non-ideal aerospike engines promise a significant payload gain.

1. Introduction

The European Space Agency (ESA) contributes with the European Service Module (ESM) to NASA's spacecraft Orion. Besides maintaining presence in low earth orbit (LEO), robotic exploration of the moon and Mars, ESA prioritizes in its Terrae Novae 2030+ Exploration Strategy Roadmap[1] for the provision of supply capacities on the moon. Part of this roadmap is the concept of the so-called European Large Logistics Lander (EL3).

To be launched on Ariane 6, EL3 should provide a payload of 1800 kg.[2] It consists of three main components: the Lunar Descent Element (LDE), the Cargo Platform Element (CPE), and the actual payload (see Tab. 1). There are already suggestions for the engine selection, e.g. a cluster of Nammo's 6kN MMH/MON RELIANCE thruster or a cluster of ArianeGroup's 5kN MMH/MON SPE-T thruster. Both engines are conventional rocket engines featuring bell-type nozzles. Although a higher system weight results, a cluster promises easier thrust throttling and reduces the propulsion system overall length.[2]

A further reduction in the overall length can be achieved by using aerospike nozzles. Unlike conventional bell-type nozzles, which expand the flow within their structure and without the influence of the environment, the flow from aerospike nozzles is expanded around a central body, with exposure to the environment. The aerospike nozzle is therefore an altitude-adaptive nozzle concept and is typically predestined for use in main or first stages.

However, the aerospike nozzle shows another very interesting property. The truncation of the spike leads to an additional rear surface on which, provided that the resulting wake flow closes, an I_{sp}-generating pressure acts. This is in contrast to a bell-type nozzle, where a trunction inevitably always leads to an I_{sp} loss. The truncation of an aerospike nozzle can be an additional benefit if done cleverly, and is therefore also interesting for an aerospike application under vacuum conditions.

Lander descent engines typically use hypergolic propellants. Their advantage is easy ignition and storability.[3] A disadvantage is their toxicity and the correspondingly complex handling required. The green propellant combination LOX/CH4 offers an easier-to-use alternative that also provides a high specific impulse. In addition, future in-situ production on other celestial bodies (e.g. Mars or asteroids) is conceivable. For this reason, LOX/CH4 is an interesting candidate for future lunar lander propellant systems.[4] In the scope of NASA's Exploration Systems Architecture Study (ESAS), several pressure fed LOX/CH4 engines with a thrust range of 20-35 kN were selected and tested in cooperation with their developers.[5,6]

The focus of this study is on the design of aerospike nozzles. Typically, aerospike nozzles are designed with an ideal contour, i.e. with a homogeneous and parallel exhaust flow, leading to the characteristic long tip. In this study also non-ideal aerospike nozzles are designed, where no tip but a stump is obtained. In both cases, mass flow and exhaust jet momentum are identical, but the non-ideal aerospike gains extra thrust from the stump surface back pressure.

Copyright © 2023 by First Author. Posted on line by the EUCASS association with permission.

DOI: 10.13009/EUCASS2023-059

Table 1: EL3 properties[2]

Payload (incl. CPE)	kg	>1800
Structural mass	kg	>1700
Initial mass	kg	9900
Diameter	m	4.57
Height LDE	m	3
Total height	m	5.96 - 18[a]

[a]Depending on Ariane 6 fairing

2. Setup and Design

The total required velocity capacity of the lander results from the sum of the necessary velocity changes. The mission scenario starts with the launch on Ariane 6, and a following direct trans lunar injection (TLI). The lander engine then takes over the apogee correction maneuver (ACM) and two firings for the polar lunar orbit injection (LOI) with 100 km of altitude. The expected velocity capacity up to this point is Δv=0.93 km/s.[2,7] Assuming a descent in the polar region, the remaining velocity after touch down is almost zero. Therefore, the velocity capacity required for descent corresponds to the previous orbital velocity of 1.63 km/s. All in all, a total requirement of 2.56 km/s must be covered by the propulsion system. This value is used to calculate the needed propellant mass. The desired engine thrust is F=30 kN or in case of a cluster F=6·5 kN.

2.1 Combustion Properties

In the past, comparable lander propulsion systems have used a pressure fed propellant supply,[4] because it is reliable and there is no need to develop turbo pumps. Therefore, a comparable combustion pressure[8] of 2 MPa was selected for the underlying design, with a LOX to LCH4 ratio of ROF=3.2.

A conventional and an aerospike engine differ in the shape of the combustion chamber. While bell-type engines feature a cylindrical combustion chamber, aerospike engines feature a ring-shaped one, which leads to a comparably heavier combustion chamber, due to the additional inner wall. To ensure comparability, both engine types were considered to feature the same combustion chamber length of 0.2 m and the same wall design principles, being convectively cooled by propellants. From experimental experience gained at DLR, the design is based on an additive layer manufacturing (ALM), made of Inconel 718, and able to withstand the expected pressures, temperatures and heat flux loads. To simplify later calculations, the thrust chambers with their cooling channels were considered to be equal to a solid wall thickness of 5 mm and the nozzle extensions with their cooling channels to be equal to 3 mm. Hence, the engines' total mass could be derived from their related surfaces. Table 2 summarizes the common engine properties.

Table 2: Comman Engine Properties

$p_{cc,tot}$	MPa	2
$T_{cc,tot}$	K	3500
κ	-	1.132
$\mathfrak{M}$	g/mol	21.305
ROF	-	3.2
A_{cc}/A_t	-	2.64
ρ_w	kg/m^3	8150[b]
$t_{w,cc}$	mm	5
$t_{w,NE}$	mm	3

[b]Inconel 718

2.2 Reference Bell Type Nozzles

A set of conventional reference engines was designed based on the engine properties given in Tab. 2. The engines featured thrust-optimized parabola nozzles (TOP) with area ratios of A_t/A_e=50, 80 and 100, respectively. Following the approach of Rao,[9] minimum length nozzles result. To decrease the propulsion system length further and in order to simply the thrust throttling, a single engine was replaced by a cluster of six small engines (see Fig. 1, left).

DOI: 10.13009/EUCASS2023-059

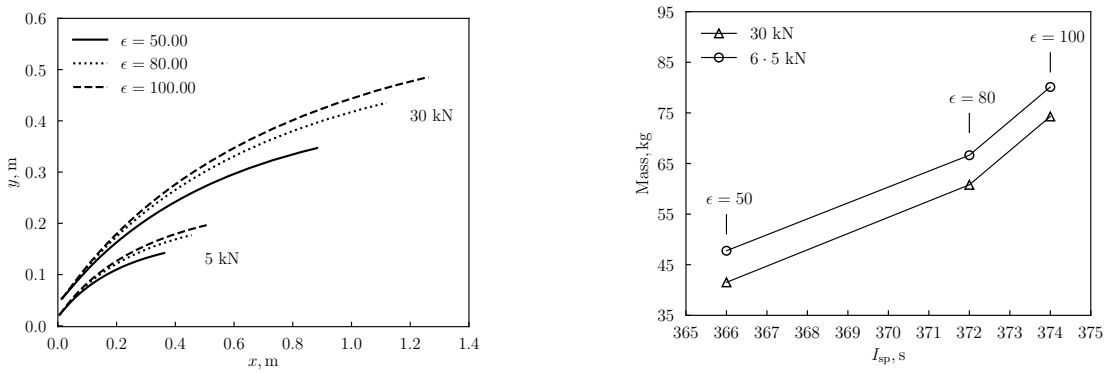

Figure 1: Conventional TOP nozzles, contours (left) and related engine masses (right)

Figure 1 (right) displays the total masses as a function of the specific impuls I_{sp}. To make it comparable to usual values, the I_{sp} was calculated using g_{Earth}. The cluster masses increased only by 7.8%-15.0% compared to the single engines. But, the diververgent part of the nozzle was significantly shortened down to 59%. Therefore in literature,[7] cluster configurations are often preferred.

2.3 Ideal Aerospike Nozzles

The ideal aerospike nozzles, designed following the approach by Angelino and Lee,[10–12] feature a uniform and parallel exit flow. In contrast, the reference TOP nozzles create a non-uniform exit flow with a radial velocity component. To design comparable aerospikes, the TOPs parabolic contours were first elongated until wall exit angles of 0° were reached (see Tab. 4). The resulting 'ideal' exit area ratios were then used to design the ideal aerospikes. After that, the obtained aerospike nozzles were truncated to the original TOP area ratios.

Table 3: TOP nozzle properties

ϵ_{TOP}	ϵ_{ideal}	$M_{e,ideal}$	$L_{\text{TOP}}/L_{\text{ideal}}$
50	50.7	4.005	0.664
80	83.3	4.276	0.596
100	105.6	4.405	0.566

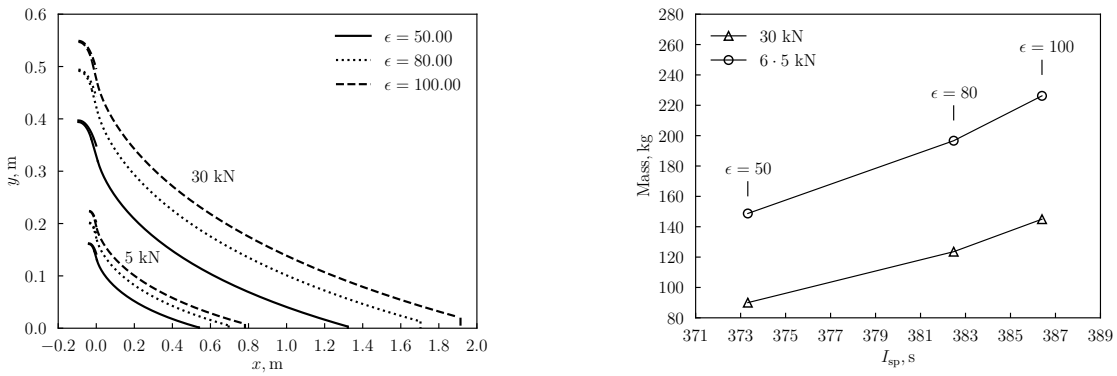

Figure 2: Ideal aerospike nozzles, contours (left) and related engine masses (right)

The question whether an external aerospike flow expansion is sufficient or whether a combined internal/external flow expansion is necessary can be answered with the desired exit Mach number M_e and the related flow deflection angle

DOI: 10.13009/EUCASS2023-059

θ derived from the Prandt-Meyer equation. Considering a maximum external deflection of 90°, a Mach Number of M_e=3.61 can be derived, corresponding to an area ratio of ϵ_{max}=24.84. It is obvious that for the given expansion ratios 50, 80 and 100, aerospike nozzles with an internal/external flow expansion are mandatory. The yet-required transition Mach number M_{tr}, where the internal expansion turns into the external expansion, corresponds to half the overall turning angle, derived from the intended exit Mach number M_e.

The design is an iterative process where the mass flow is adjusted until the target thrust of 30 kN is reached. As for the reference TOPs, in Fig. 2 (right), the engine masses of the single engines and the clusters are given as a function of the specific impulse I_{sp}. The cluster masses increase 56-65% compared to the single aerospike engines. For the mass calculations, the properties given in Tab. 2 were used. The achieved length reduction (cluster vs. single engine) is 59% for all expansion ratios (Fig. 2, left).

2.4 Non-Ideal Aerospike Nozzles

The non-ideal aerospike nozzles are designed to feature the same target thrust of F=30 kN as the ideal ones. The nozzles differ in the shape of the exit surface, which is a ring instead of a disc. As a result, the contour no longer merges the symmetry axis, but now forms a stump. To design these nozzles, the outer radius of the ring is increased as a percentage of the initial ideal disc radius.

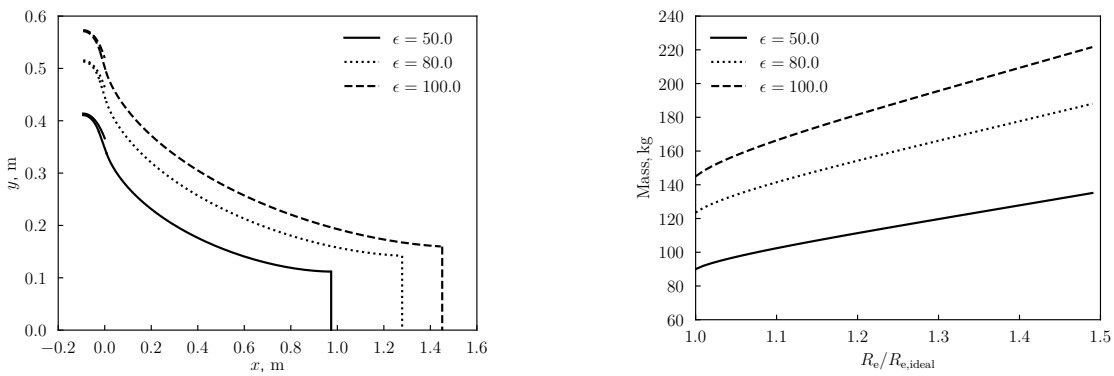

Figure 3: Non-ideal aerospike nozzles, contours for $R_e/R_{e,ideal}$=1.05 (left) and related engine masses (right)

Figure 3 (left) shows the obtained contours of the single aerospike engines for an outer radius increase of 5%. It turned out that a slight increase in the outer radius lead to a considerable rear surface. An additional benefit was the accompanying length reduction. Here it was 24% for all expansion ratios. In combination, the opposing effects led to a mass increase that is still acceptable (Figure 3, right).

2.5 Base Pressure

Suitable models are required to estimate the thrust contribution of the rear surface with its closed wake. Appropriate approaches can be found in the literature. Fick and Schmucker,[13] for example, compared and developed several models from cold gas tests. Figure 4 shows two of the compared models, together with experimental data. Their empirical model of supersonic cylinder flow shows the best agreement with the data. Also included is another model developed by Lamb and Oberkampf.[14] It delivers results that come close to the experimental data, too. In addition, Fick and Schmucker found that for a truncation of 12-16%, the arithmetic average value of the exit pressure of the ideal and the truncated aerospike nozzle fits the data well.[13]

DOI: 10.13009/EUCASS2023-059

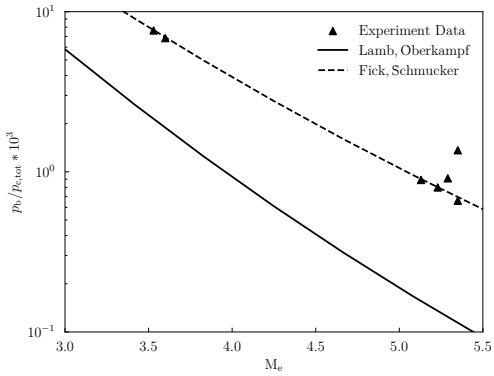

Figure 4: Base pressure models

3. Results and Discussion

First, the impact of the spike truncation on the I_{sp} and the engine mass was examined for the single engines, without considering the rear surface base pressure. The mass flow of the respective engine was varied iteratively until the target thrust of F=30 kN was reached. The truncation of the spike led to an increase of the throat area and thus to an increase of the engine diameter.[15]

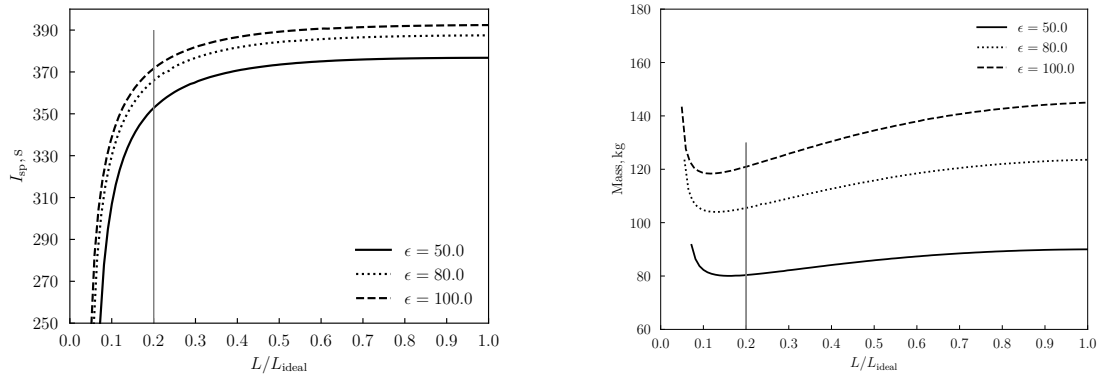

Figure 5: Truncated ideal aerospike nozzles, I_{sp} (left) and related engine masses (right)

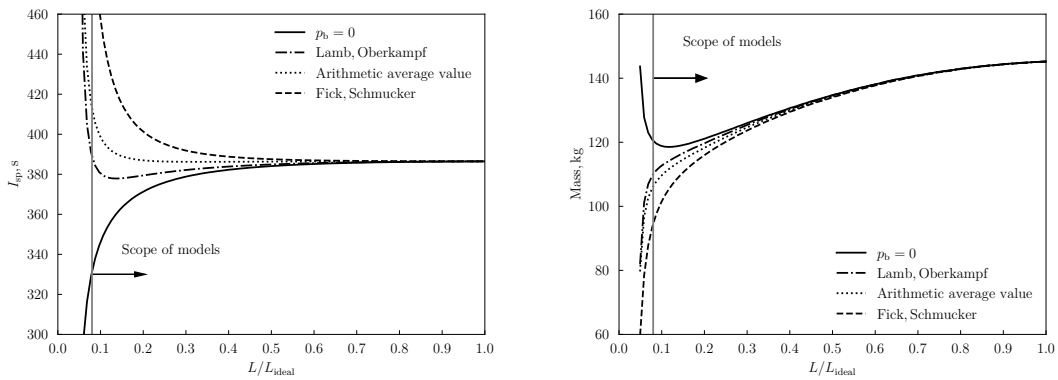

Figure 6: Truncated ideal ϵ=100 aerospike nozzle including base pressure, I_{sp} (left) and related engine masses (right)

DOI: 10.13009/EUCASS2023-059

Figure 5 shows that as the truncation progresses, the engine mass decreases more than the I_{sp}. It turns out that a reduction down to L/L_{ideal}=0.4 is possible with almost no losses. In addition, it can be seen that from $L/L_{ideal} \approx$ 0.05-0.08, the motor mass increases significantly again due to the truncation. So far, the literature recommendations[15,16] to truncate the spike to L/L_{ideal}<0.2 (gray line) cannot be confirmed.

These results change when the base pressure is taken into account. Due to the closed wake, a positive thrust component is achieved. Considering the constant target thrust, the I_{sp} increases, the fuel mass flow decreaes, and as a result the engine mass decreases. Figure 6 reveals the relations for different base pressure models. The I_{sp} as well as the engine mass are shown again. For a clearer overview, the comparison is limited to the engine with the area ratio of ϵ=100. However, the results are qualitatively transferrable to other area ratios.

While the impact of the base pressure on the I_{sp} becomes significant for L/L_{ideal}<0.6 (Fig. 6, left), the impact on the engine mass becomes noticeable below L/L_{ideal}<0.5 (Fig. 6, left). The models themselves show different results. The model by Lamb and Oberkampf achieves the most conservative values, followed by the arithmetic mean value of the ideal and truncated exit pressure. The model by Fick and Schmucker provides the most significant base pressure component.

All models clarify the significant impact on I_{sp} increase and engine mass reduction of the additional thrust that is caused by the base pressure. The presented base pressure models are only experimentally validated for exit Mach numbers M_e>3.5 which is marked in Fig 6.

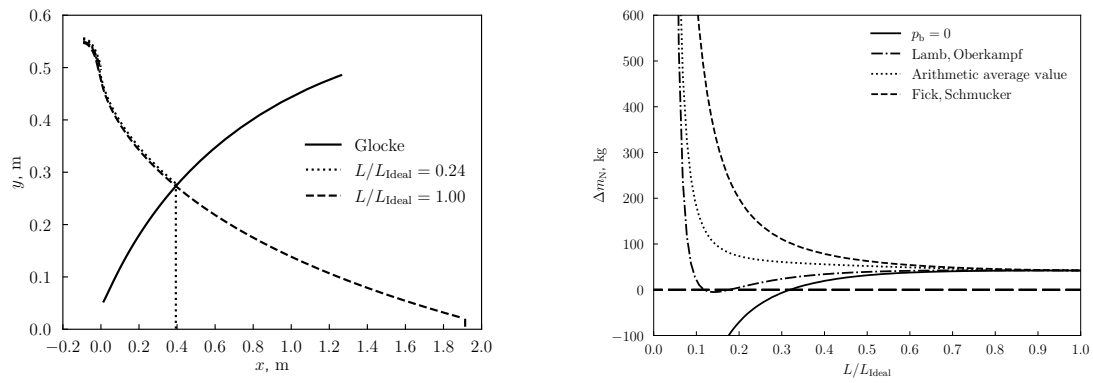

Figure 7: Comparison of TOP and aerospike nozzle, both ϵ=100, contours (left) and payload gain (right)

The increase of the I_{sp}, and thus the reduction of the propellant mass flow, as well as the reduction of the engine mass, increase in combination the payload capacity of the lunar lander. Figure 7 (left) shows the contour comparison of a single 30 kN aerospike engine with the conventional reference engine with a TOP nozzle, each with ϵ=100. The trend of the related payload gain Δm_N in Fig. 7 (right) is very similar to the trend of the I_{sp}: it increases with the spike truncation. Considering the model, a payload gain of 75-200 kg is possible for a truncation down to 20%. In relation to the intended total payload of 1800 kg (Tab. 1), this means an increase of 4.2-11.1%.

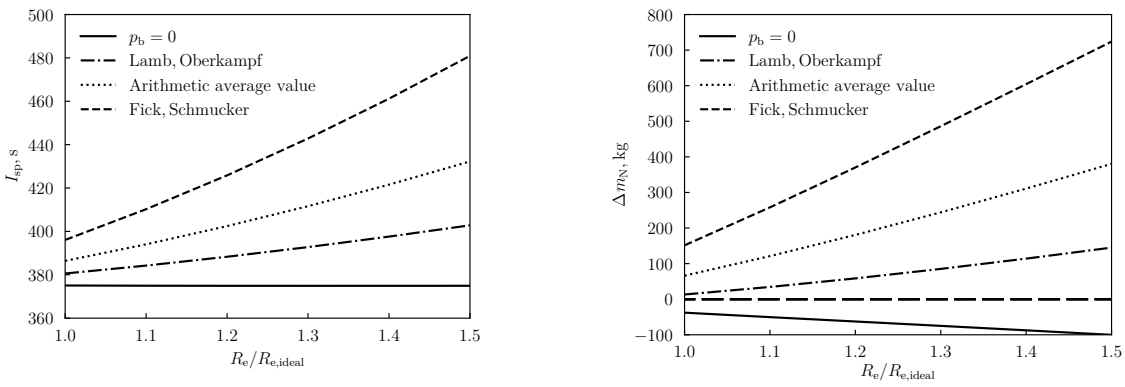

Figure 8: Trucated non-ideal ϵ=100 aerospike nozzle (20%), I_{sp} (left) and related payload gain (right)

Due to their increased rear surface, the non-ideal aerospike nozzles feature additional performance. Figure 8 (left)

DOI: 10.13009/EUCASS2023-059

reveals the I_{sp} increase of a non-ideal ϵ=100 aerospike, being truncated to 20% as well. Although of course the engine mass also increases with increasing rear surface, the I_{sp} increase remains dominant, leading to a significant payload gain. Figure 8 (right) shows the potential of the non-ideal aerospike nozzle concept. A payload gain of more than 200 kg (or 11.1%) seems quite possible. Table 4 gives some values gained from Fig. 8 (right).

Table 4: Payload gain of non-ideal aerospike engine with 20% truncation

$R_e/R_{e,ideal}$	Δm_N, %
1.0	4.2 - 11.1
1.1	6.7 - 14.3
1.2	9.7 - 20.6

It should be mentioned here that a 50% increase ($R_e/R_{e,ideal}$=1.5) in the engine diameter to around 1.8 m would still be realistic compared to the EL3 overall diameter of 4.57 m (see Tab. 1).

4. Conclusions

The aim of the study was not to provide absolute values but to compare the results of different configurations in a sufficient good quality. The following points can be derived:

∘ Replacing a central conventional engine with a cluster of several small ones makes sense, considering the significant reduction in system length.
∘ Aerospike engines inherently shorten the propulsion system.
∘ A cluster of aerospike engines is too heavy. A single aerospike engine should be preferred.
∘ Due to the rear surface back pressure, truncated aerospike engines offer an I_{sp} increase, resulting in a payload gain.
∘ Non-ideal aerospike nozzles with their enlarged rear surface increase the I_{sp} gain again.
∘ Payload gains of over 10% are possible.

It should be noted that the study aimed to reveal the I_{sp} benefit of an increased aerospike rear surface. The challenges arising from the enlargement of the necessary annular combustion chamber are not taken into account. A cluster of conventional cylindric combustion chambers is conceivable here, of which the adjoining divergent nozzle sections change their cross section from a disk to a curved slit-like shape. In any case, it is necessary for the wake flow to close in order to produce the described effect.
Nonetheless, annular chambers would offer the application of performance-enhancing rotational detonation techniques (RDE). The next steps are experimental studies to validate the base pressure models, especially for the non-ideal aerospike nozzles.

5. Acknowledgments

The authors like to thank J. van Schyndel and Dr. J. Riccius supporting the thrust chamber design. Special thanks to C. Morris.

References

[1] European Space Agency, *Terrae Novae 2030+ Strategy Roadmap*, 2022.

[2] L. Duvet, A. Cropp, P. Hager, K. Nergaard, N. Gollins. European Access to the Lunar Surface: EL3. *72nd International Astronautical Congress (IAC)*, 2021.

[3] R. W. Orloff. Apollo by the numbers: A statistical reference. *NASA history series*, NASA and History Office, 2000.

[4] J. R. Simmons. Design and Evaluation of Dual-Expander Aerospike Nozzle Upper Stage Engine. *Ph.D. Thesis*, Wright Patterson Air Force Base, 2014.

DOI: 10.13009/EUCASS2023-059

[5] J. B. Olansen. Morpheus: Advancing Technologies for Human Exploration. *Tech. Rep.*, GLEX-2012.05.2.4x12761, NASA, United States, 2012.

[6] J. Collins, E. Hurlbert, C. Romig, J. Melcher, A. Hobson, P. Eaton. Sea-Level Flight Demonstration and Altitude Characterization of a LO2/LCH4 Based Ascent Propulsion Lander. *45th AIAA/ASME/SAE/ASEE Joint Propulsion Conference & Exhibit*, 2009.

[7] M. Landgraf, L. Duvet, A. Cropp, G. Alvarez, G. Ambroszkiewicz, M. Bottacini, P. Brunner, L. Bucci, W. Carey, A. Casini, G. Cifani, O. Dubois-Matra, J. Ellwood, A. Gonzáles Fernández, A. Gernoth, A. Getemis, G. Gomez, D. Greuel, P. Hager, G. Magistrati. Autonomous Access to the Moon for Europe: The European Large Logistic Lander. *72nd International Astronautical Congress (IAC)*, Proceedings, 2022.

[8] M. D. Klem, T. D. Smith, M. F. Wadel, M. L. Meyer, J. M. Free, H. A. Ill. Liquid oxygen/liquid methane propulsion and cryogenic advanced development. *62nd International Astronautical Congress (IAC)*, 6256-6267, 2011.

[9] G. V. R. RAO. Exhaust Nozzle Contour for Optimum Thrust. *Journal of Jet Propulsion*, **28**, 6:377-382, 1958.

[10] G. Angelino. Approximate method for plug nozzle design. *AIAA Journal*, **2**, 10:1834-1835, 1964.

[11] C. C. Lee. Fortran programs for plug nozzle design. *Tech. Rep., Brown Engineering Company, inc.* for George C. Marshall Space Flight Center, Huntsville, Alabama, 1963.

[12] F. Ditsche. Entwurf einer Aerospike-Düse für ein 500 N - Lachgas/Ethan (N2O/C2H6) - Triebwerk. *Master Thesis*, TU Berlin-Institut für Luft- und Raumfahrt, Berlin, 2022.

[13] M. Fick, R. H. Schmucker. Performance aspects of plug cluster nozzles. *Journal of Spacecraft and Rockets*. **33**, 4:507-512, 1996.

[14] J. P. Lamb, W. L. Oberkampf. Review and development of base pressure and base heating correlations in supersonic flow. *Journal of Spacecraft and Rockets*. **32**, 1:8-23, 1995.

[15] T. J. Mueller, W. P. Sule, A. E. Fanning, T. Giel, F. L. Galanga. Analytical and Experimental Study of Axisymmetric Truncated Plug Nozzle Flow Fields. *Tech. Rep.*, UNDAS TN-6012-FR-10, University of Notre Dame for NASA, 1972.

[16] F. B. Lary. Advanced Cryogenic Rocket Engine Program, Aerospike Nozzle Concept Volume 1. *Tech. Rep.*, AFRPL-TR-67-280, North American Rockwell Corporation, 1968.

[17] S. Bartel. Designstudie eines 30 kN-LOX/LCH4-Aerospike-Triebwerks für einen Mond-Lander. *Thesis*, University of Applied Sciences Aachen, 2023.